2015 48th Hawaii International Conference on System Sciences

Rapid Assessment, Visualization and Mitigation of Cascading Failure Risk in Power Systems

Pooya Rezaei
School of Engineering
University of Vermont
Burlington, VT
pooya.rezaei@uvm.edu

Margaret J. Eppstein
Department of Computer Science
University of Vermont
Burlington, VT
Maggie.Eppstein@uvm.edu

Paul D. H. Hines
School of Engineering
University of Vermont
Burlington, VT
paul.hines@uvm.edu

Abstract

This paper describes a new approach, using "Random Chemistry" sampling, to estimate the risk of large cascading blackouts triggered by multiple contingencies. On a 2383 bus test case the new approach finds the expected value of large-blackout sizes (a measure of risk) two orders of magnitude faster than Monte Carlo sampling, without introducing measurable bias. We also derive a method to compute the sensitivity of blackout risk to individual component-failure probabilities, allowing one to quickly identify low-cost strategies for reducing risk. For example, we show how a 1.9% increase in operational costs reduced the overall risk of cascading failure in a 2383-bus test case by 61%. An examination of how risk changes with load yielded a surprising decrease in cascading failure risk at the highest loadings, due to increased locality in generation and less long-distance transmission. Finally, this paper proposes new visualizations of spatio-temporal patterns in cascading failure risk that could provide valuable guidance to system planners and operators.

1. Introduction

Cascading failure risk estimation is a notoriously difficult problem, because of the many complicated processes involved, the combinatorial number of possible triggering events, and the fact that cascade sizes tend to have a power-law tail [1], [2], [3], [4]. And yet, because of the critical importance of electric power systems, which are increasingly exposed to hazards (storms, earthquakes, terrorists, etc.), cascading failure risk analysis is necessary. Recognizing this need, the North American Reliability Council (NERC) has adopted rules requiring electric utilities to study cascading failure risk [5].

Existing approaches to the cascading failure risk analysis problem in power systems can be categorized as: high-level statistical methods (such as branching processes) [6], [7], [8], [9], [10], [11], [12], abstracted topological models [13], [14], [15], [16], optimization-based approaches [17], [18], [19], [20], [21], and detailed sampling/simulation methods (such as Importance Sampling and the Splitting Method) [22], [23], [24], [25], [26]. Each of these approaches has advantages, but also important limitations. Statistical approaches provide high-level insight, but can abstract away potentially critical information, such as the sensitivity of risk to particular component failure probabilities. Purely topological models are relatively easy to use, but can be misleading [27]. Existing optimization approaches can provide guaranteed levels of performance, but are largely limited to tractable linearized models, which may obscure important non-linear dynamics. Previous sampling methods are powerful in that they can typically be applied to general (linear or non-linear) models, but often provide only a modest speedup over simple Monte-Carlo sampling (see, e.g., [25]).

Recently, we proposed a new sampling method, referred to as Random Chemistry (RC), that can find minimal $n-k$ contingencies that cause large blackouts in $O(\log(n))$ simulations [28]. In [29] we outlined a method for using RC to estimate cascading failure risk, based on the expected size of blackouts in various size ranges. This paper describes the new approach, and compares its speed to standard Monte Carlo risk estimation. In addition, this paper describes and illustrates a method for estimating the sensitivity of the overall risk of cascading failure to individual component failure probabilities and shows how risk changes as a function of load in a 2383-bus test case. Finally, we explore new methods for mitigating and visualizing cascading failure risk that could be beneficial to both planners and operators.

1530-1605/15 $31.00 © 2015 IEEE
DOI 10.1109/HICSS.2015.331

2. Methods

2.1. Random Chemistry (RC) Algorithm

The RC algorithm is a stochastic set-size reduction search strategy that can be used to efficiently (in logarithmic time) find minimal subsets that are associated with a certain outcome of interest. RC is a "wrapper"-type global search method that can be used with any forward simulator capable of detecting outcomes of interest; the algorithm was first developed and applied to genome wide association analysis in [30], and was recently adapted to the problem of finding minimal $n-k$ blackout-initiating contingencies (henceforth referred to as "malignancies") in power grids [28].

Briefly, in the context of power grids, the RC algorithm operates as follows. In the first step, we use a cascading failure simulator (to date, we have used DCSIMSEP [28], [31]) to randomly search for a large $n-k_{\text{init}}$ contingency m that results in a large blackout. For this paper, we define n to be the number of branches in the system and we only consider branch outages. The proposed method can easily be adapted to include other types of contingencies, such as generator outages. If k_{init} is sufficiently large (we used $k_{\text{init}} = 80$), this step typically requires very few tries. The algorithm then stochastically reduces m according to a logarithmically decreasing set size reduction schedule (we currently use $\{k_{\text{init}} = 80,\ k_2 = 40,\ k_3 = 20,\ k_4 = 14,\ k_5 = 10,\ k_6 = 7,\ k_{\text{final}} = 5\}$) by testing random subsets of the desired size until one is found that causes a large blackout. If no such subset is found within a prespecified maximum number of tries T (we currently use $T = 20$), the run is restarted from a new random $n - k_{\text{init}}$ contingency. Once the RC algorithm finds a blackout causing $n - k_{\text{final}}$ contingency, the contigency set of size k_{final} is exhaustively searched until a minimal $n-k$ malignancy[1] is identified of size $2 \leq k \leq k_{\text{final}}$ (in [28] we searched starting from $k = 4$ and worked down to $k = 2$, but here we first search all $k = 2$ contingencies, in random order, and then work up to $k = 4$, if needed). This cycle can then be repeated to obtain large collections of minimal $n-k$ malignancies.

2.2. Using RC to Estimate Risk

While the RC algorithm can quickly generate large collections of minimal blackout-causing contingencies (malignancies), it does not directly produce measures of blackout risk that can allow one to compare different cases, as one can do with standard Monte Carlo reliability analysis procedures. This section describes a method (based on [29]) to use RC to produce this type of risk metric. Specifically, we focus on estimating the expected value of large cascading-blackout sizes triggered by exogenously-caused $n-k$ branch (transmission line or transformer) outage contingencies.

First, we start with a network model for a system at an $n-1$ secure state x and some simulator $S(c,x)$ that gives the size of the blackout that results from an arbitrary $n-k$ contingency c. Second, we set a threshold T_S, which encodes our definition for "large blackout", where any m such that $S(m,x) \geq T_S$ is considered a malignancy. This threshold is selected by the user, based on the minimum size of the blackout they wish to consider as "large". In [28] we considered a large blackout to occur when at least 10% of the nodes became separated from the rest of the grid. In this work we set $T_S = 5\%$ of system load and then examine the risk due to blackouts of various sizes above this minimum threshold. Third, we run the RC algorithm repeatedly, which will find some fraction of the minimal $n-\{2...k_{\max}\}$ malignancies in the system, for some $k_{\max} \leq k_{\text{final}}$. Let $\Omega_{RC,k}$ be the set of minimal $n-k$ malignancies found by RC, and Ω_k is the set of minimal $n-k$ malignancies that exist in the particular test case being studied, for each $k \in \{2...k_{\max}\}$. Finally, given the data that result, one can estimate the risk of large cascading failures $\hat{R}_{RC}(x)$ at a given system state x with:

$$\hat{R}_{RC}(x) = \sum_{k=2}^{k_{\max}} \frac{\hat{M}_k}{|\Omega_{RC,k}|} \sum_{m \in \Omega_{RC,k}} \Pr(m) S(m,x) \quad (1)$$

where $\hat{M}_k$ denotes an estimate of $|\Omega_k|$, the size of the set Ω_k, and $\Pr(m)$ is the occurrence probability for a specific malignancy m. As more iterations of RC are completed, (1) will capture the risk from an increasingly large collection of $n-\{2...k_{\max}\}$ malignancies.

It is important to note that (1) assumes that the size of a blackout triggered by any superset of a malignancy m is the same as $S(m,x)$. This assumption is needed because RC finds minimal malignancies, but our risk estimate needs to incorporate risk from both minimal and non-minimal ones. For example, if the set of components $\{23, 48\}$ is a minimal malignancy, (1) also needs to account for the risk from $\{23, 48, 72\}$ (and all other supersets of $\{23, 48\}$). Assuming that $S(m,x)$ is the same as $S(m',x)$, where $m' \supset m$, allows us to incorporate the risk from all of the supersets m' without having to explicitly run them through the simulator, and does not appear to introduce measurable bias into the outcome (based on comparisons with

[1] A minimal $n-k$ malignancy is defined as a set of k components that initiate a large cascading blackout when they fail (nearly) simultaneously, but if any one of the k components did not fail a blackout would not result.

Monte Carlo sampling, as shown in Sec. 4-A). See [29] for more details on the impact of this assumption on risk assessment.

In addition, the results in this paper assume that branch outages are statistically independent when computing $\Pr(m)$. Extending the approach to account for correlations in outage probabilities is possible, but remains for future work.

A unique aspect of the cascading failure problem is that the risk due to disturbances that impact one city are very different from blackouts that spread across a large region, such as Aug. 14, 2003 [32]. It is therefore useful to separately estimate risk from blackouts in various size ranges. Separating the risk estimate from (1) into the portions contributed by blackouts in various size ranges is relatively straightforward. For example, the risk from blackouts with sizes between 20% and 30% of load can be found by summing over only those malignancies m for which $20\% \leq S(m,x) < 30\%$ of load. Sec. 4-C illustrates this by showing trends in risk for blackouts in different size ranges for our test case.

2.3. How many contingencies cause blackouts?

In order to use (1) to estimate risk, one needs an estimate of the number of minimal malignancies that cause large blackouts. Specifically, we need to find $\hat{M}_k \sim |\Omega_k|$ for $k \in \{2...k_{\max}\}$. In [28], we estimated $|\Omega_k|$ using a moving window approach to averaging the empirically observed rate at which the RC algorithm is finding new malignancies for each given k. However, the resulting estimates are noisy and can take a long time to converge. In more recent experimentation we have found that fitting an exponential model to the number of unique malignancies found by RC yields more accurate estimates more quickly.

To illustrate why an exponential model is appropriate, consider a jar of N balls numbered $1, 2...N$. If balls are removed from the jar one at a time (and then replaced), it can be shown (see Appendix) that the expected number of uniquely numbered balls drawn after i draws (N_i) follows:

$$N_i = N(1 - e^{i \ln(1-\frac{1}{N})}) \tag{2}$$

If, in the RC case, every malignancy was uncovered with equal probability during the course of the algorithm, then least-squares fitting of (2) to data for i and N_i could be used to find an estimate for N. However, subsequent experimentation has indicated that, because some components appear in malignancies orders-of-magnitude more frequently than others (see [28]), the probability of drawing each malignancy is not uniform. As a result, the data for i and N_i in the RC case fall slightly below the curve in (2), but are still exponential in shape.

Based on these observations, we suggest an alternative exponential model, which was empirically found to be more accurate for our application. Specifically, we found that the number of unique malignancies found by RC can be represented by the Cumulative Distribution Function (CDF) of the exponential Weibull distribution. We thus use a non-linear least squares method to fit the parameters λ, μ, ν, and $\hat{M}_k$ (the latter being the estimate of $|\Omega_k|$ and the variable of interest) in the relationship:

$$|\Omega_{RC,k}(i_k)| \sim \hat{M}_k \left(1 - e^{-(\frac{i_k}{\lambda})^{\mu}}\right)^{\nu} \tag{3}$$

where i_k is the total number of (not necessarily unique) minimal $n-k$ malignancies found so far by the RC algorithm and, as in (1), $|\Omega_{RC,k}(i_k)|$ is the number of unique minimal $n-k$ malignancies found.

2.4. Using RC to Identify Critical Components

In [28], we observed that the RC algorithm could be used to identify critical components based on the number of potential malignancies in which they occur. Here we improve on that by using the risk estimate in (1) to find the sensitivities of overall risk to individual component failures. If p_i is the outage probability for component i then one can use the partial derivative of $\hat{R}_{RC,k}(x)$ with respect to each p_i as a measure of the sensitivity of the overall risk caused by $n-k$ malignancies to this component, and then sum this over all $k \in \{2..k_{\max}\}$, as follows:

$$\frac{\partial \hat{R}_{RC,k}}{\partial p_i} = \frac{\hat{M}_k}{|\Omega_{RC,k}|} \sum_{m \in \Omega_{RC,k}} S(m,x) \frac{\partial}{\partial p_i} \Pr(m) \tag{4}$$

$$\frac{\partial \hat{R}_{RC}(x)}{\partial p_i} = \sum_{k=2}^{k_{\max}} \frac{\partial \hat{R}_{RC,k}(x)}{\partial p_i} \tag{5}$$

If we assume that outages are independent then, for any particular malignancy m that includes branch i:

$$\frac{\partial}{\partial p_i} \Pr(m) = \frac{\Pr(m)}{p_i} \tag{6}$$

Section 4-C shows the resulting sensitivities from (5) for the test case used in this paper.

3. Test case

The results in this paper come from experiments with a model of the 2004 peak winter load in the Polish power system (available with MATPOWER [33]). This

test case has 2383 buses, $n = 2896$ branches (transmission lines and transformers), and 24.6 GW of total load. Some of the transmission lines were overloaded in the original system. In order to remove these overloads and ensure that the system was initially $n-1$ secure, we increased the original line flow limits to be the larger of the existing limit and 1.05 times the pre-contingency line flows that occur when the system is at 1.10 times the actual load; we refer to this case, before adjusting the dispatch, as the "baseline case."

To explore how cascading failure risk changes as a function of load (presented in Sec. 4-C), we prepared pre-contingency versions of the test system at a variety of load levels, ranging from 50% to 115% of the baseline case load. For each load level, a preventative security constrained dc optimal power flow (SCOPF) was used to dispatch generators, while maintaining $n-1$ security (see [34] for SCOPF implementation details).

4. Experiments, Results and Discussion

This section describes results from several experiments designed to illustrate the properties of our approach.

4.1. Computational efficiency

The first experiment compares the computational effort needed to compute blackout risk using the RC method, with the computational cost of standard Monte Carlo risk estimation.

To obtain data from RC, we applied RC to the 100% load (baseline) case; a total of 1 million RC runs yielded 123,883 unique minimal $n-\{2,3,4,5\}$ malignancies causing $S \geq 5\%$ load loss. This included all 540 $n-2$ malignancies (subsequently verified by exhaustive search), 38,212 $n-3$ malignancies, 67,483 $n-4$ malignancies and 17,648 $n-5$ malignancies. The estimate of $\hat{M}_2$ by (3) correctly identified the total number of $n-2$ malignancies (Fig. 1a) and $\hat{M}_3$ appears to be converging (Fig. 1b). Based on this estimate, we believe the 38,212 $n-3$ minimal malignancies found represent approximately 57% of the full set Ω_3.

Because it is not (currently) feasible to accurately estimate $\hat{M}_4$ or $\hat{M}_5$, subsequent risk calculations used only the data from the identified $n-2$ and $n-3$ minimal malignancies. Note that the impact of this assumption on the risk estimate is small for two reasons. First, the probabilities ($\Pr(m)$) of $n-4$ and $n-5$ malignancies are extremely low (especially when outages are assumed to be independent). More importantly, because each term $\Pr(m)S(m,x)$ in (1) simultaneously

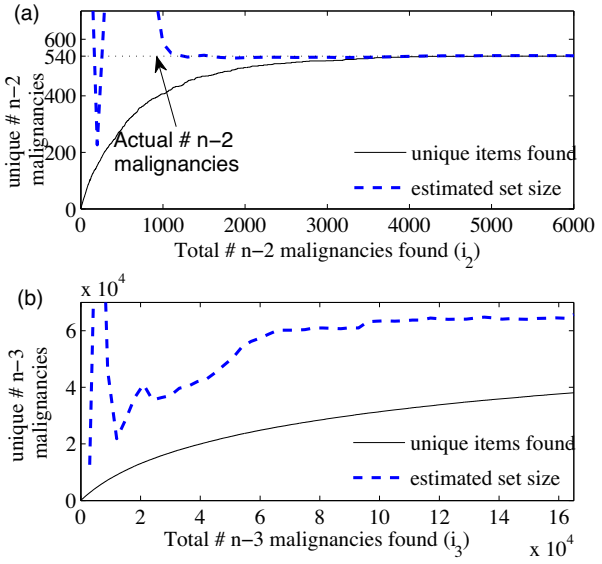

Fig. 1. The number of unique minimal $n-k$ malignancies found by RC in the test system, as a function of the total number of minimal $n-k$ malignancies found by RC at 100% load, and the estimate of the set size ($\hat{M}_k$) by Eq. (3) for (a) $k=2$ and (b) $k=3$.

captures risk from a minimal malignancy and all of its supersets, the results from (1) already include the contributions from $\sim 3\times10^9$ $n-4$ and $\sim 7\times10^{12}$ $n-5$ malignancies. Only the minimal $n-4$ and $n-5$ malignancies are neglected; we conjecture that there are few of these, relative the many non-minimal $n-4$'s and $n-5$'s.

The resulting cascading failure risk estimate from (1), with $k_{\max}=3$, converges to the same value as standard Monte Carlo (MC) estimates for the baseline case, but RC is at least 2 orders of magnitude faster. Note that while the RC risk estimate quickly converges after about 100,000 calls to the simulator, the three MC estimates have still not completely converged after 20 million calls to the simulator (Fig. 2). On a 2.66 GHz Intel Core i7 MacBook Pro with 8 GB memory, it took an average of approximately 0.4 seconds per call to DCSIMSEP for this test system; thus, if run serially, it would require approximately 11 hours of CPU time for the RC risk estimate to converge on this system, whereas the MC risk estimate would still not have completely converged after 92 days. However, the proposed approach can easily be parallelized; we ran independent simulations in parallel on a cluster of 100 cores. With sufficient computational resources, the current approach can be used for day-ahead planning even for large systems; we plan additional modifications that may enable real-time updates of risk.

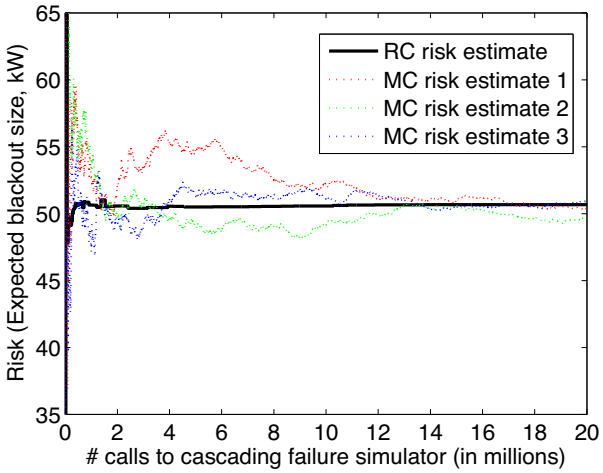

Fig. 2. RC risk estimates for the test system at 100% load, as computed by Eq. (1), compared to three risk estimates using Monte Carlo (MC) sampling.

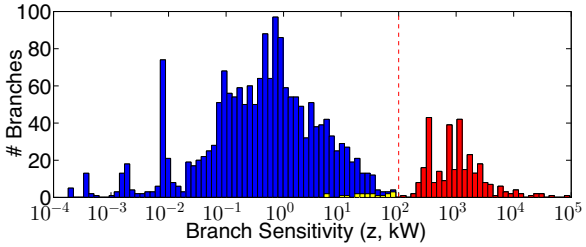

Fig. 3. Histogram of branch sensitivities for the baseline test case, calculated from (5).

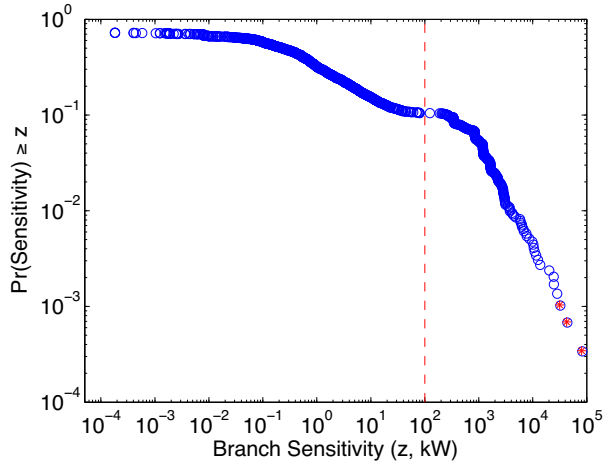

Fig. 4. Complementary cumulative distribution function of branch sensitivities for the baseline test case, from. (5).

4.2. Sensitivity of risk to individual components

In the baseline test case, we found that individual branch sensitivities from (5) follow a largely bimodal distribution (see Fig. 3; note that the x-axis is on a logarithmic scale). There were 307 branches that exhibited sensitivities above 100 kW, (red bars in Fig. 3) with the remainder of the branches contributing relatively little to risk. Closer examination revealed that all of the sensitivities above 100 kW were caused by branches that occurred in $n-2$ malignancies, reflecting the fact that the contribution of minimal $n-3$ malignancies to overall cascading failure risk is small, at least when outages are assumed to be independent. A few branches that occurred in only one or two minimal $n-2$ malignancies, each resulting in relatively small cascades, had sensitivities < 100 kW (yellow bars, Fig. 3), but the majority of the components with sensitivity < 100 kW occurred in $n-3$, but not in $n-2$ minimal malignancies (blue bars, Fig. 3).

In Fig. 4 we plot the cumulative complementary distribution function (CCDF) of the branch sensitivities; the change in slope in the CCDF at 100 kW corresponds to the change in modes in the distribution of branch sensitivities above and below 100 kW illustrated in Fig. 3. The CCDF of branches with sensitivity > 100 kW follows a roughly power-law distribution (Fig. 4).

It is interesting that there is only a weak correlation between branch risk sensitivity and pre-contingency flows, with no bimodality present in the distribution of the latter (Fig. 5). Except for the most heavily loaded branches, pre-contingency flow is not a strong predictor

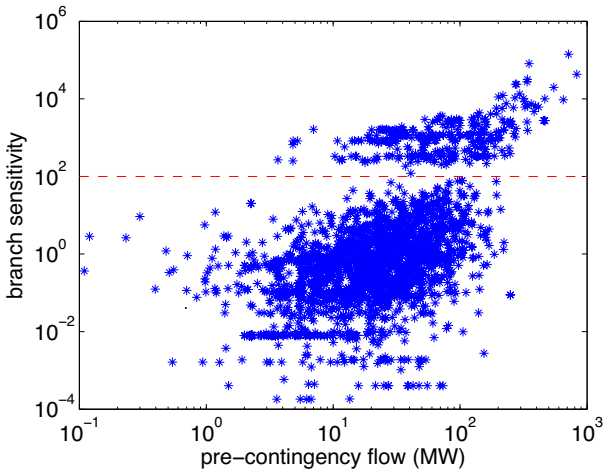

Fig. 5. Branch sensitivities for the baseline test case shown as a function of (absolute) pre-contingency power flow.

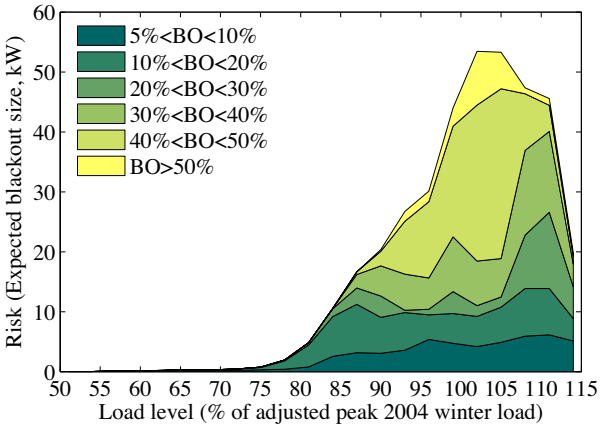

Fig. 6. RC risk of various blackout (BO) sizes as a function of load level for the test system with pre-contingency dispatch by SCOPF.

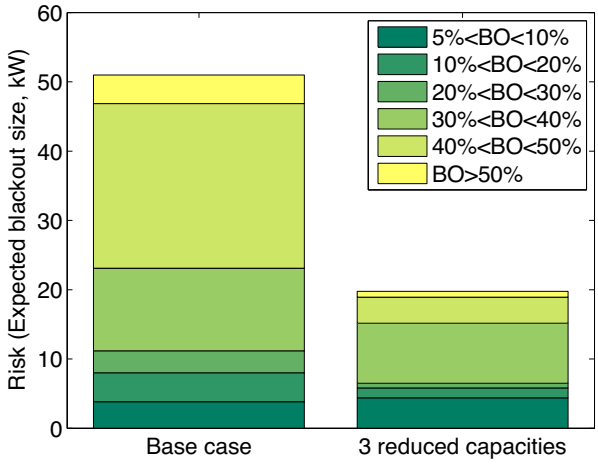

Fig. 7. Cascading failure risk at 100% load before and after decreasing the flow limits on the three most "sensitive" branches.

of individual branch sensitivities. On the other hand, the lines that contribute most to blackout risk are generally those with very large power flows, which makes sense given that all of the power flowing over a line will be re-distributed throughout the system after the line trips.

4.3. Risk vs. load

Examining risk as a function of load using the SCOPF-dispatched cases (see Sec. 3) yielded some surprising results. The risk of very large blackouts ($S \geq 40\%$), calculated from (1), increases quickly above 85% load, but then decreases above 105% load (Fig. 6). Inspection of the resulting data indicate that the reduced risk at higher load levels results from the way that SCOPF uses more local generation with less long-distance transmission at higher load levels.

To illustrate this, Table I shows the total amount of pre-contingency power flow on the largest transmission branches in the system. At 105% load, these lines carry 17,102 MW, whereas at 115% load the total flow is reduced to 15,916 MW.

TABLE I. Total (absolute) power flow on branches with pre-contingency flow ≥ 200 MW.

Load level	95%	100%	105%	110%	115%
MW flow	16,312	17,032	17,102	16,869	15,916

4.4. Risk mitigation

Here we describe results that illustrate how the proposed approach can be used to identify strategies for reducing risk.

Motivated by the observation that a large portion of the risk comes from a small number of components, and that the total flow on the largest transmission lines seems to correlate with risk, we reran SCOPF for the 100% load case after (temporarily) reducing the line limits for the three most sensitive branches by a factor of two (branches 96, 23, and 169, shown with red asterisks in Fig. 4), and then re-estimated RC risk on the re-dispatched system (but with the original line limits restored). The resulting system had a modest 1.6% increase in dispatch cost (a projected increase of $33,300/hr) but resulted in a 61% reduction in overall cascading failure risk and, importantly, an 83% reduction in the risk of very large blackouts $S \geq 40\%$ (Fig. 7). This result suggests that using the risk estimation methods proposed here could be used to design new optimal power flow formulations that could better balance the trade-offs between operating costs and large-blackout risk.

4.5. Comparing adjacent load levels

An examination of how the contingencies change in the test system as the load is increased revealed that there is (not surprisingly) a high probability that a minimal $n-2$ malignancy present at a given load level is also present at a load level that is 1% lower or higher (Fig. 8, solid circles and squares, respectively). Specifically, for load levels between 55% and 115% in the test system, the conditional probability that a given $n-2$ malignancy is present at a given load averages 0.89 and 0.82 if the same malignancy was present at 1% lower or 1% higher load, respectively. In contrast, the

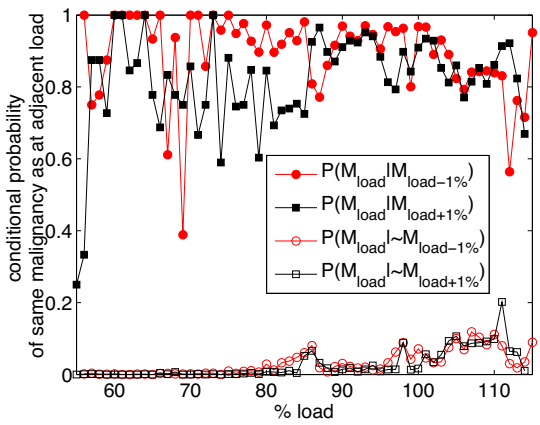

Fig. 8. Conditional probabilities of a minimal $n-2$ malignancy being present in the test system at a given load, given that it was (solid markers) or was not (open markers) present in the same system at 1% lower load (red circles) or 1% higher load (black squares).

conditional probability that a malignancy is present at a given load if it was *not* present at 1% lower or higher load (Fig. 8, open circles and squares, respectively) averages only 0.03 and generally rises as load increase ($p < 1e\text{-}9$). The similarity in these lower two curves in Fig. 8 shows that new minimal malignancies are just as likely to appear in the test system if one reduces the load by 1% than if one raises the load by 1%; this is presumably due to changes in load distributions due to changes in generator dispatch by SCOPF. In future work, we will explore whether one can take advantage of the relatively high consistency in malignancies at similar system loads to permit rapid updating of risk in response to real-time changes in load.

4.6. Visualization

Sampling approaches to cascading failure risk analysis, such as RC, produce large amounts of spatially-explicit and state-specific data, including which $n-k$ contingencies can lead to cascading failure, which branches or generators have the greatest sensitivities, how spatial patterns of risk change with the state of the system, etc. Presenting such Big Data in a way that provides actionable insight to grid planners and operators is a challenging topic in and of itself. For example, while Fig. 8 indicates that there is generally high persistence of malignancies between similar loadings, it does not elucidate that there can be large changes in the spatial patterns of malignancies at different load levels. In contrast, the visualization in Fig. 9a-d makes these patterns obvious; here, the gray network in the foreground indicates branches in the Polish system, while the black network in the background connects the branch pairs in all of the $n-2$ malignancies for (a) 75% load, (b) 85% load, (c) 100% load, and (d) 115% load. This type of network visualization could be interactively augmented in several useful ways, such as coloring the branches based on load level, proportion of load capacity, or branch risk sensitivity, or coloring or sizing the $n-2$ malignancy links based on size of the resulting cascading failure, etc., in response to planner or operator preferences. Such visualizations might give planners and operators an immediate sense of the overall level of risk of cascading failure as well as identifying which regions of the grid are more at risk and which components are the most sensitive. Note how the spatial pattern of risk shifts for different levels of load when generators are dispatched according to SCOPF, with some branches becoming more sensitive and others less sensitive as load is increased. If we draw the same figure for the SCOPF case at 100% load, after reducing the capacity of the three most sensitive branches, the number of $n-2$ malignancies drops from 540 to 320, as shown in Fig.10.

A complementary type of visualization could be used to alert grid operators as to potential malignancies in response to real-time outages. For example, supposing that branch 96 fails (Fig. 11, marked by a black asterisk). For load levels {90%, 100%, 105%, 115%} there are {6, 146, 191, 40} $n-2$ malignancies that involve branch 96, so the system is no longer $n-1$ secure, and if any of these other branches (thick red lines in Fig. 11a-d, respectively) fails it will trigger a large cascading failure. (Note that the reduction from 191 to 40 $n-2$ malignancies at 105% and 115%, respectively, is due to more local generation at the higher load level, which reduces the loading on long distance lines, as described in Section 4-C.) Real-time displays of this type of $(n-1)-1$ information in response to component failures (e.g., in a storm) could provide valuable information to operators as to how to best respond to real-time contingencies to reduce the risk of cascading failure. As described above, this type of visualization could be augmented to contain additional information through the coloring or sizing of nodes and edges.

5. Conclusions and Future Work

This paper presents a new computationally efficient method, based on the Random Chemistry (RC) algorithm in [28], for estimating the risk of large (e.g., $\geq 5\%$ of system load) cascading blackouts. A compari-

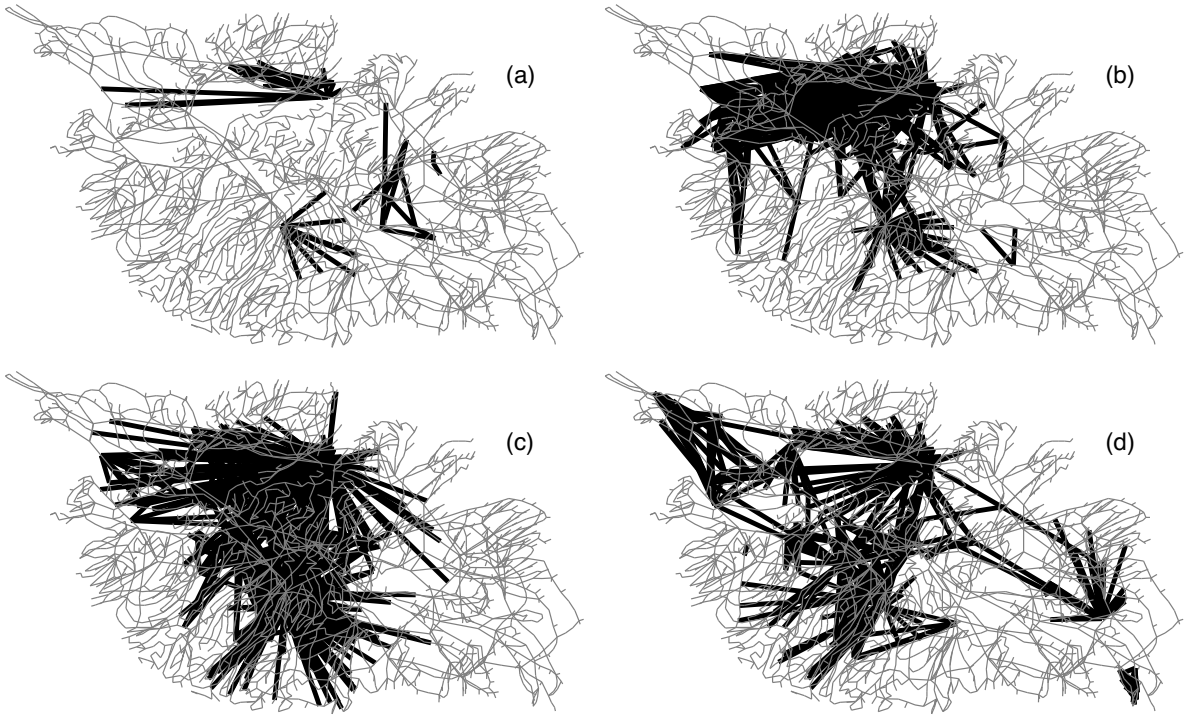

Fig. 9. The test system with branches in gray: $n-2$ malignancies are shown in black for (a) Load level 75%, 39 $n-2$ malignancies, (b) load level 85%, 345 $n-2$ malignancies, (c) load level 100%, 540 $n-2$ malignancies, (d) load level 115%, 378 $n-2$ malignancies.

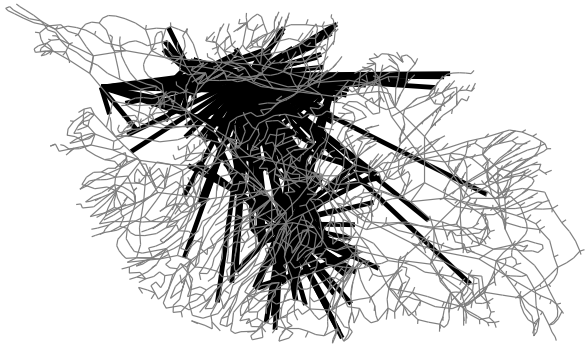

Fig. 10. The test system with branches in gray: $n-2$ malignancies are shown in black for the 320 $n-2$ malignancies that occur at 100% load when dispatch is generated using SCOPF with branch capacities halved for branches 96, 23, and 169 (compare to base capacities at 100% load in Fig. 9c.

son of this method to Monte Carlo (MC) simulation on a model of the Polish transmission system shows that the new approach is at least two orders of magnitude faster than MC, and does not introduce measurable bias into the estimate.

The computational efficiency of the RC approach comes from the way that it is able to find large blackout-causing contingencies in $O(\log(n))$ simulations, as opposed to MC, which samples broadly from all possible contingencies, of which only a tiny fraction cause cascading failures. Since the size of blackouts follows a roughly scale-free distribution [35], the probability of finding a large blackout by random sampling decreases dramatically with the size of the blackout. Thus, RC becomes increasingly efficient relative to MC when searching for larger blackouts. In future work we plan to relax the assumption of independence of component outages and to incorporate additional efficiencies into RC risk estimation that will make this method fast enough for both day-ahead planning and real-time updating of cascading failure risk estimates.

Here, we assume that branch failures in initiating malignancies occur simultaneously. In future work, we will explore the impact of order of initiating contingencies on risk. It should also be noted that the RC risk estimation algorithm is independent of the cascading simulator employed. To date, we have used DCSIMSEP [28], [31], which does not consider dynamic instabilities, voltage collapse, or transient instabilities (all of which may contribute to blackouts) nor does it con-

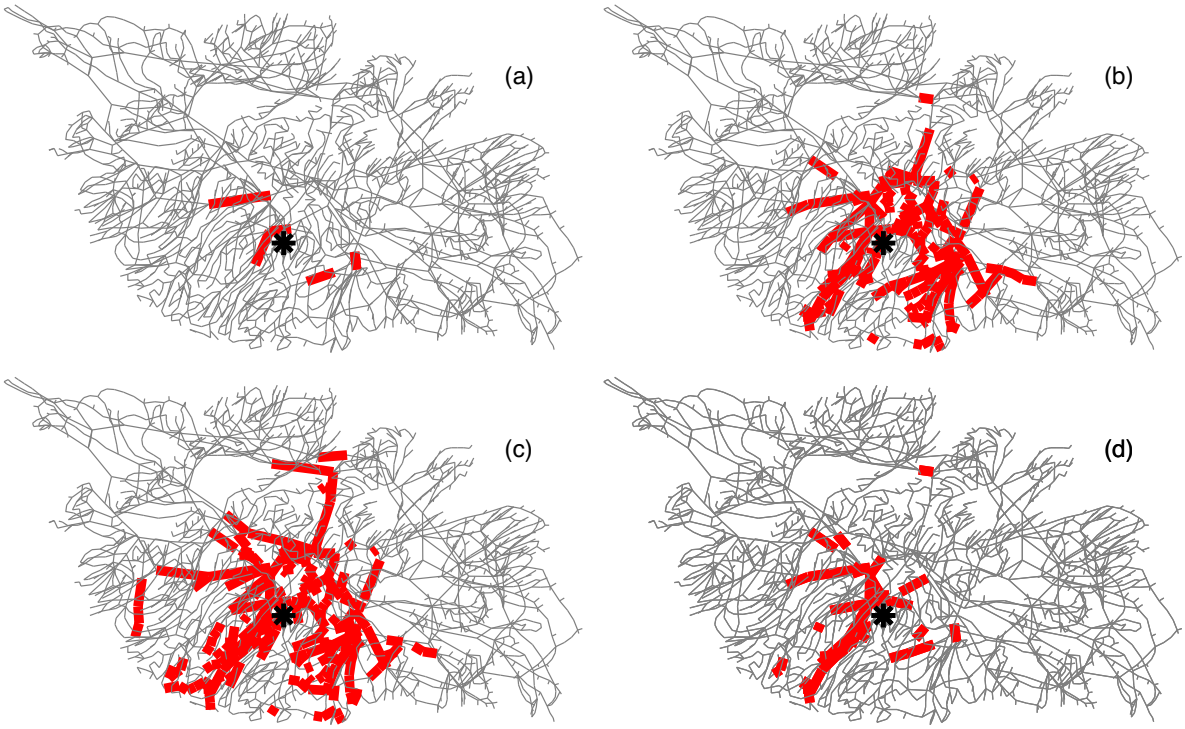

Fig. 11. The test system with branches in gray, a single branch outage marked by a black asterisk, and individual branch outages that would cause a cascading failure shown in thick red lines for: (a) 90% load, (b) 100% load, (c) 105% load, and (d) 115% load.

trol cascades (e.g., by regulation reserve or automated voltage regulation). However, the risk analysis process proposed here can be used in combination with any cascading failure simulator that reports the blackout size, given an initiating contingency. In future work we will incorporate a more detailed cascading failure simulator and test the impact of those phenomena on the efficiency of the proposed approach.

When examining how the risk of cascading failure changes with system load level, we found that risk can sometimes decrease as load increases. This was found to be due to increased use of local generation at the highest load levels, which resulted in reduced power flows on large long-distance transmission lines; this illustrates the importance of understanding how spatial patterns in generator dispatch affect cascading failure risk. In future work, we will also explore how spatially heterogeneous changes in load may impact the risk of cascading failure.

Using RC also enables us to disaggregate risk with respect to the resulting blackout sizes and the sensitivity of blackout risk to individual branch outage probabilities. We derived a method to use the data generated by the RC approach to quickly estimate the sensitivity of risk to particular components. We illustrated the potential value of this knowledge by showing how one could mitigate risk by dispatching generators to limit the flows on some of the most sensitive branches. Specifically, for a model of the Polish system at peak 2004 winter load, we dispatched generators based on the assumption that the capacities of the three branches with the highest risk sensitivity were half of their true values. The result was a 61% reduction in the overall risk of large blackouts ($\geq 5\%$ of system load) and an 83% reduction in the risk of very large blackouts ($\geq 40\%$ of system load), but only a modest 1.9% increase in operational costs. As the risks and costs of large cascading failures increase, planners could similarly employ the RC method to weigh the tradeoffs between economic operational efficiency and blackout risk, and adjust optimal power flow formulations accordingly.

Finally, we introduced new visualizations of the spatio-temporal patterns in cascading failure risk as the state of the system changes. We believe that such visualizations could provide valuable guidance to system planners and operators in seeking to minimize and mitigate the risk of cascading failures.

Appendix: Derivation of Equation (2)

This appendix presents the derivation of (2), the expected number of uniquely numbered objects found (N_i) after i draws from a jar of N objects numbered $1...N$.

After the first draw, one will have found precisely 1 unique object. In subsequent draws, the expected number of unique items found is:

$$N_i = N_{i-1} + \frac{N - N_{i-1}}{N} = rN_{i-1} + 1 \qquad (7)$$

where $r = 1 - \frac{1}{N}$. Equation (7) is a recursive function, for which we would like to find a closed-form expression. To do so, one can divide both sides by r^i, which gives:

$$\frac{N_i}{r^i} = \frac{N_{i-1}}{r^{i-1}} + \frac{1}{r^i} \qquad (8)$$

Let

$$\mathcal{N}_i = \frac{N_i}{r^i} \qquad (9)$$

Then:

$$\mathcal{N}_i = \mathcal{N}_{i-1} + \frac{1}{r^i} \qquad (10)$$

$\mathcal{N}_0 = 0$, so:

$$\mathcal{N}_i = \sum_{j=1}^{i} \frac{1}{r^j} = \frac{N\left(1 - r^i\right)}{r^i}$$

Based on (9): $N_i = N\left(1 - r^i\right) = N(1 - e^{i\ln(r)})$, as presented in (2).

References

[1] B. A. Carreras, D. E. Newman, I. Dobson, and A. B. Poole, "Evidence for Self-Organized Criticality in a Time Series of Electric Power System Blackouts," *IEEE Transactions on Circuits and Systems–I: Regular Papers*, vol. 51, no. 9, pp. 1733–1740, 2004.

[2] I. Dobson, K. R. Wierzbicki, J. Kim, and H. Ren, "Towards quantifying cascading blackout risk," in *2007 iREP Symposium - Bulk Power System Dynamics and Control - VII, Revitalizing Operational Reliability*, (Charleston SC, USA), Aug. 2007.

[3] P. Hines, J. Apt, and S. Talukdar, "Large blackouts in north america: Historical trends and policy implications," *Energy Policy*, vol. 37, pp. 5249–5259, 2009.

[4] M. M. Vaiman, *et al.*, "Risk assessment of cascading outages: Methodologies and challenges," *IEEE Transactions on Power Systems*, vol. 27, no. 2, pp. 631–641, 2012.

[5] NERC, "Standard TOP-004-2: Transmission Operations," standard, North American Electric Reliability Corporation, 2007.

[6] H. Ren and I. Dobson, "Using transmission line outage data to estimate cascading failure propagation in an electric power system," *Circuits and Systems II: Express Briefs, IEEE Transactions on*, vol. 55, pp. 927 –931, sept. 2008.

[7] I. Dobson, J. Kim, and K. R. Wierzbicki, "Testing branching process estimators of cascading failure with data from a simulation of transmission line outages," *Risk Analysis*, vol. 30, pp. 650–662, Apr. 2010.

[8] J. Kim and I. Dobson, "Approximating a loading-dependent cascading failure model with a branching process," *IEEE Transactions on Reliability*, vol. 59, pp. 691 –699, dec. 2010.

[9] I. Dobson, "Estimating the propagation and extent of cascading line outages from utility data with a branching process," *IEEE Transactions on Power Systems*, vol. 27, no. 4, pp. 2146–2155, 2012.

[10] M. Chertkov, F. Pan, and M. Stepanov, "Predicting failures in power grids: The case of static overloads," *Smart Grid, IEEE Transactions on*, vol. 2, pp. 162–172, March 2011.

[11] H. Wu and I. Dobson, "Cascading stall of many induction motors in a simple system," *Power Systems, IEEE Transactions on*, vol. 27, pp. 2116–2126, Nov 2012.

[12] M. Rahnamay-Naeini, Z. Wang, N. Ghani, A. Mammoli, and M. Hayat, "Stochastic analysis of cascading-failure dynamics in power grids," 2014.

[13] R. Albert, I. Albert, and G. Nakarado, "Structural vulnerability of the north american power grid," *Physical Review E*, vol. 69, p. 025103(R), Feb 2004.

[14] S. V. Buldyrev, R. Parshani, G. Paul, H. E. Stanley, and S. Havlin, "Catastrophic cascade of failures in interdependent networks," *Nature*, vol. 464, pp. 1025–1028, 2010.

[15] C. D. Brummitt, R. M. D'Souza, and E. A. Leicht, "Suppressing cascades of load in interdependent networks," *Proceedings of the National Academy of Sciences*, vol. 109, March 2012.

[16] J. Yan, H. He, and Y. Sun, "Integrated security analysis on cascading failure in complex networks," *Information Forensics and Security, IEEE Transactions on*, vol. 9, pp. 451–463, March 2014.

[17] D. Bienstock and A. Verma, "The n-k problem in power grids: New models, formulations, and numerical experiments," *SIAM Journal on Optimization*, vol. 20, no. 5, pp. 2352–2380, 2010.

[18] D. Bienstock, "Optimal adaptive control of cascading power grid failures," Preprint: arXiv:1012.4025v1, arXiv, 2010.

[19] D. Bienstock, G. Grebla, and G. Zussman, "Optimal control of cascading power grid failures with imperfect flow observations," in *SIAM Workshop on Network Science (NS14)*, Jul 2014.

[20] V. Donde, V. Lopez, B. Lesieutre, A. Pinar, C. Yang, and J. Meza, "Severe multiple contingency screening in electric power systems," *IEEE Transactions on Power Systems*, vol. 23, pp. 406–417, May 2008.

[21] A. Pinar, J. Meza, V. Donde, and B. Lesieutre, "Optimization strategies for the vulnerability analysis of the electric power grid," *SIAM Journal on Optimization*, vol. 20, no. 4, pp. 1786–1810, 2010.

[22] R. Billinton and W. Li, "A system state transition sampling method for composite system reliability evaluation," *IEEE Transactions on Power Systems*, vol. 8, pp. 761 – 770, Aug. 1993.

[23] K. Bae and J. S. Thorp, "A stochastic study of hidden failures in power system protection," *Decision Support Systems*, vol. 24, no. 3, pp. 259–268, 1999.

[24] D.S. Kirschen *et al.*, "A probabilistic indicator of system stress," *IEEE Transactions on Power Systems*, vol. 19, no. 3, pp. 1650–1657, 2004.

[25] Q. Chen and L. Mili, "Risk-based composite power system vulnerability evaluation to cascading failures using importance sampling," in *Proc. of the IEEE Power and Energy Society General Meeting*, (Detroit), 2011.

[26] J. Kim, J. Bucklew, and I. Dobson, "Splitting method for speedy simulation of cascading blackouts," *IEEE Transactions on Power Systems*, vol. 28, no. 3, pp. 3010–3017, 2013.

[27] P. Hines, E. Cotilla-Sanchez, and S. Blumsack, "Do topological models provide good information about vulnerability in electric power networks?," *Chaos: An interdisciplinary journal of nonlinear science*, vol. 20, no. 3, 2010.

[28] M. Eppstein and P. Hines, "A "Random Chemistry" algorithm for identifying collections of multiple contingencies that initiate cascading failure," *IEEE Transactions on Power Systems*,

vol. 27, no. 3, pp. 1698–1705, 2012.
[29] P. Rezaei, P. D. H. Hines, and M. Eppstein, "Estimating cascading failure risk with random chemistry," *IEEE Transactions on Power Systems*, vol. (in review; pre-print: http://arxiv.org/abs/1405.4213), 2014.
[30] M.J. Eppstein *et al.*, "Genomic mining for complex disease traits with "Random Chemistry"," *Genetic Programming and Evolvable Machines*, vol. 8, no. 4, pp. 395–411, 2007.
[31] P. Hines, "DCSIMSEP: A simulator of cascading separation in power grids. http://uvm.edu/~phines/dcsimsep/."
[32] USCA, "Final Report on the August 14, 2003 Blackout in the United States and Canada," tech. rep., US-Canada Power System Outage Task Force, 2004.
[33] R. Zimmerman, C. Murillo-Sánchez, and R. Thomas, "MATPOWER: Steady-state operations, planning, and analysis tools for power systems research and education," *IEEE Transactions on Power Systems*, vol. 26, pp. 12 –19, feb. 2011.
[34] P. Rezaei and P. Hines, "Changes in cascading failure risk with generator dispatch method and system load level," in *IEEE PES Transmission and Distribution Conference and Exposition*, pp. 1–5, 2014.
[35] D. E. Newman, B. A. Carreras, V. E. Lynch, and I. Dobson, "Exploring complex systems aspects of blackout risk and mitigation," *Reliability, IEEE Transactions on*, vol. 60, no. 1, pp. 134–143, 2011.